JOURNAL OF GEOPHYSICAL RESEARCH, VOL. 112, D11309, doi:10.1029/2006JD008008, 2007

Quantification of the factors controlling tropical tropospheric ozone and the South Atlantic maximum

B. Sauvage,[1] Randall V. Martin,[1,2] A. van Donkelaar,[1] and J. R. Ziemke[3]

Received 8 September 2006; revised 24 January 2007; accepted 8 February 2007; published 13 June 2007.

[1] We quantify the processes controlling the tropical tropospheric ozone burden with particular attention to the tropical Atlantic, using a global chemical transport model (GEOS-Chem) constrained by satellite and in situ observations of O_3, NO_2, and HCHO. Lightning is the dominant contributor to tropical tropospheric O_3, accounting for more than 37% of the O_3 burden over the Atlantic on annual average. The contributions from biomass burning, soils, and fossil fuels are 4 to 6 times smaller, despite comparable source strengths. This discrepancy can be explained by the tropical ozone production efficiency of lightning (32 mol/mol), soils (14 mol/mol), biomass burning (10 mol/mol), and fossil fuel (13 mol/mol) sources, as calculated using sensitivity simulations with a 1% perturbation. The role of volatile organic compound emissions on the tropical Atlantic ozone burden is negligible (<2.5%). Stratosphere-troposphere exchange accounts for less than 5% of the regional O_3 burden. The tropical Atlantic O_3 burden is more strongly influenced by nitrogen oxides from Africa (>30%) than from South America (>18%) or the eastern tropics (>11%). Lightning is responsible for more than 39% of the atmospheric oxidation capacity, higher than other sources. The dominant sources of uncertainty in the tropical oxidation rate are the lightning magnitude and the cloud convective parameterization.

Citation: Sauvage, B., R. V. Martin, A. van Donkelaar, and J. R. Ziemke (2007), Quantification of the factors controlling tropical tropospheric ozone and the South Atlantic maximum, *J. Geophys. Res.*, *112*, D11309, doi:10.1029/2006JD008008.

1. Introduction

[2] The tropical troposphere largely controls the oxidation capacity and radiation budget of the global atmosphere. Ozone (O_3) plays a key role in the global oxidizing power of the atmosphere, as the main producer of OH, the primary atmospheric oxidant [*Thompson*, 1992]. Ozone production is driven by the supply of nitrogen oxides from lightning, biomass burning, fossil fuel combustion, and soils [*Jacob et al.*, 1996]. Dynamics also strongly influence photochemistry, forcing convergence in the lower troposphere, and vertical ascent of air masses through deep convection into the upper troposphere where chemical species have a longer lifetime, and can be redistributed globally. We use a global chemical transport model to disentangle these processes by interpreting satellite retrievals of tropical tropospheric O_3.

[3] Tropical tropospheric O_3 columns have been inferred from a number of instruments including the GOME [*Burrows et al.*, 1999], and the OMI [*Levelt et al.*, 2006], and MLS instruments [*Waters et al.*, 2007]. The GOME instrument onboard the European Remote Sensing-2 satellite provided continuous global monitoring of O_3 atmospheric columns through observation of solar backscatter over 1995–2003. GOME observes the atmosphere in the nadir view with a 40 km along track by 320 km across track horizontal resolution. Daily tropospheric O_3 retrievals have been performed by *Liu et al.* [2005]. The OMI and MLS instruments were launched in July 2004 onboard the Aura spacecraft. OMI is a nadir-scanning instrument that detects backscattered solar radiance to measure the O_3 column with near global daily coverage at a resolution of up to 13 km × 24 km at nadir. The MLS instrument is a thermal-emission microwave limb sounder that measures vertical profiles of O_3 in the mesosphere, the stratosphere, and the upper troposphere from limb scans [*Froidevaux et al.*, 2007]. Daily tropospheric O_3 columns have been retrieved by *Ziemke et al.* [2006] by combining measurements from both MLS and OMI. The measurement uncertainty for both retrievals is 5–8 Dobson units (DU).

[4] The middle and upper troposphere of the tropical Atlantic exhibits a persistent ozone maximum as part of the well-known zonal wave-one [*Fishman et al.*, 1990; *Logan and Kirchhoff*, 1986; *Thompson et al.*, 2003]. At this altitude, ozone is critical for the global warming earth system, with maximum positive radiative effect [*de F. Forster and Shine*, 1997]. Numerous studies have attempted to understand the origin of that ozone maximum, giving evidence of various influence by the different regional sources, such as biomass burning [*Pickering et al.*, 1996; *Edwards et al.*, 2003; *Jenkins*

[1]Department of Physics and Atmospheric Science, Dalhousie University, Halifax, Nova Scotia, Canada.
[2]Also at Atomic and Molecular Physics Division, Harvard-Smithsonian Center for Astrophysics, Cambridge, Massachusetts, USA.
[3]Goddard Earth Sciences and Technology, University of Maryland Baltimore County, Maryland, USA.

0148-0227/07/2006JD008008$09.00

and Ryu, 2004b; *Sauvage et al.*, 2006], biogenic sources [*Meyer-Arnek et al.*, 2005], lightning [*Thompson et al.*, 2000; *Martin et al.*, 2002; *Jenkins and Ryu*, 2004a], dynamics [*Krishnamurti et al.*, 1993, 1996], long-range transport [*Chatfield et al.*, 2004], as well as stratospheric-tropospheric exchange [*Weller et al.*, 1996]. *Moxim and Levy* [2000] through model analysis quantified the tropospheric mass of NO_x transported into that region during September. More recently *Wang et al.* [2006] have suggested that both the Hadley and Walker circulation can contribute to the zonal wave-one pattern.

[5] Despite these accomplishments, many critically important gaps remain in our knowledge of the tropical tropospheric ozone, the Atlantic ozone maximum, and atmospheric oxidation. For instance, there has been no quantitative estimation of the different sources contributing to the annual O_3 maximum. Indeed, such analysis implies the use of a thoroughly evaluated global chemical transport model, with an accurate emission inventory of O_3 precursors, such as NO_x. Moreover, no study to date has addressed the contribution of each source to OH concentrations. The short OH lifetime (around 1 s) results in a chemical rather than transport control dependence [*Bloss et al.*, 2006]. *Manning et al.* [2005] suggest a recent 20% decrease in global OH concentrations. *Labrador et al.* [2004] find that global mean OH is highly sensitive to the NO_x from lightning. A decadal rise in OH simulated with the MOZART-2 chemical transport stems from an increase in lightning NO_x [*Fiore et al.*, 2006]. Determining processes controlling the abundance of OH are then critical to understand how the oxidation capacity of the troposphere is changing.

[6] To address these outstanding questions, we use a three-dimensional global chemical transport model (GEOS-Chem), with emissions of NO_x (lightning, biomass burning, soils) and volatile organic compounds (biomass burning) constrained by in situ and satellite observations [*Sauvage et al.*, 2007]. The emission inventory in that simulation has been validated with in situ measurements from aircraft (MOZAIC), and ozonesondes (SHADOZ) as well as GOME satellite measurements over the tropics. The resultant simulation provides a useful tool to fully understand the ozone maximum over the Atlantic. A summary of that simulation is given in section 2.

[7] The purpose of this paper is (1) to conduct sensitivity studies on NO_x emissions with a global chemical transport model to understand the processes controlling tropical tropospheric O_3 and the maximum over the South Atlantic, and (2) to quantify the influence of different sources and regions on the South Atlantic. We will address these specific points in section 3, after providing in section 2 an overview of the chemical transport model and developments by *Sauvage et al.* [2007]. Finally, we estimate errors in the factors controlling tropical tropospheric O_3 in section 4.

2. Description of the Simulation and Methodology

[8] We use the global chemical transport model (GEOS-Chem, *Bey et al.* [2001], http://www-as.harvard.edu/chemistry/trop/geos/index.html) driven with GEOS-4 meteorological fields for the year 2000. The GEOS-Chem model includes a detailed simulation of tropospheric O_3-NO_x-hydrocarbon chemistry as well as of aerosols and their precursors. The model presently includes sulfate, nitrate, ammonium, black and organic carbon, mineral dust and sea salt [*Park et al.*, 2004; *Park et al.*, 2005; *Alexander et al.*, 2005; *Fairlie et al.*, 2007]. The aerosol and gaseous simulations are coupled through formation of sulfate and nitrate, $HNO_3(g)/NO_3^-$ partitioning of total inorganic nitrate, heterogeneous chemistry on aerosols [*Jacob et al.*, 1999; *Evans and Jacob*, 2005], and aerosol effects on photolysis rates [*Martin et al.*, 2003]. The stratosphere to troposphere flux of O_3 in the model of 500 Tg/yr is prescribed by the synthetic ozone method [*McLinden et al.*, 2000].

[9] The model version used here is based on version 7-02-04 with substantial improvements in emissions and heterogeneous chemistry by *Sauvage et al.* [2007] as summarized below. The spatial distribution of lightning is scaled to reproduce seasonal mean lightning flash rates from the lightning imaging sensor and optical transient detector satellite instruments [*Christian et al.*, 2003] to improve the spatial distribution of lightning in the model. Emissions of lightning NO_x remain linked to deep convection following the parameterization of *Price et al.* [1997] with vertical profiles from *Pickering et al.* [1998] as implemented by *Wang et al.* [1998]. The magnitude of the global lightning source is 6.0 Tg N/yr of which 3.3 Tg N/yr is within 24°S–24°N. The evaluation of ozone vertical profiles conducted by *Sauvage et al.* [2007] at all tropical sites as part of the Measurement of Ozone and Water Vapor by Airbus In-service Aircraft (MOZAIC) and Southern Hemisphere Additional Ozonsondes (SHADOZ) programs has shown that the local redistribution of lightning emissions reduces the original model bias by 5–20 ppbv, versus the in situ O_3 measurements in the upper troposphere.

[10] *Sauvage et al.* [2007] also applied tropospheric NO_2 and HCHO columns from GOME as top-down constraints on emission inventories of NO_x from soils and biomass burning, and VOCs emitted from biomass burning. Biomass burning emissions include 7 Tg N/yr as NO, 4 Tg C/yr as HCHO, and 27 Tg C/yr as lumped alkenes. The soil source of 9 Tg N/yr is from *Jaeglé et al.* [2005]. The top-down constraints on emissions reduced model biases in the lower troposphere by 5–20 ppb versus in situ observations from MOZAIC program and SHADOZ network.

[11] Uptake of HO_2 on biomass burning aerosol was disabled based on recent laboratory [*Thornton and Abbatt*, 2005] and field measurements [*Yamasoe et al.*, 2000]. Uptake of HNO_3 was implemented with a reaction probability of 0.1 as measured by *Hanisch and Crowley* [2003]. These two updates to the heterogeneous chemistry improved the lower tropospheric O_3 simulation by 5 ppbv versus MOZAIC observations in biomass burning and desert regions [*Sauvage et al.*, 2007].

[12] The evaluation by *Sauvage et al.* [2007] of the tropical simulation compared to MOZAIC and SHADOZ in situ data demonstrated the capability to represent the main tropospheric ozone features. The simulation generally reproduces MOZAIC and SHADOZ tropical O_3 profiles to within 5 to 10 ppbv. GOME observations are well simulated for NO_2 ($r^2 = 0.86$, bias = 2×10^{14} molecules cm^{-2}) and HCHO ($r^2 > 0.6$, bias = 6×10^{14} molecules cm^{-2}).

[13] We use this improved simulation to assess the budget and origin of tropical (24°S–24°N) O_3 with particular attention to the South Atlantic (24°S–0°/35°W–10°E). Sensitivity studies are conducted by perturbing the main

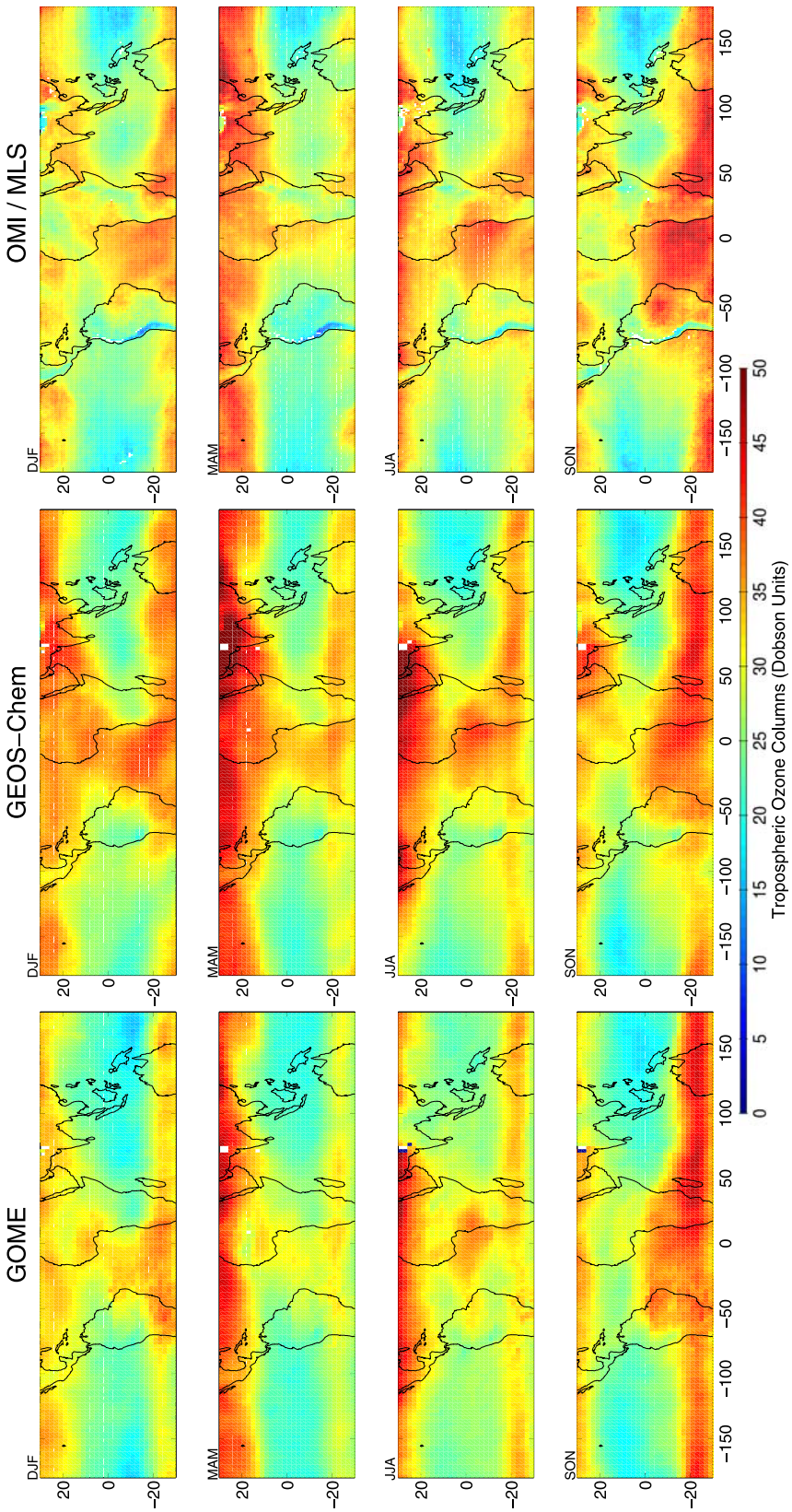

Figure 1. Seasonal tropospheric ozone columns (DU), as seen by GOME for the year 2000 (left), GEOS-Chem for the year 2000 (middle), and OMI/MLS for 2004–2005 (right).

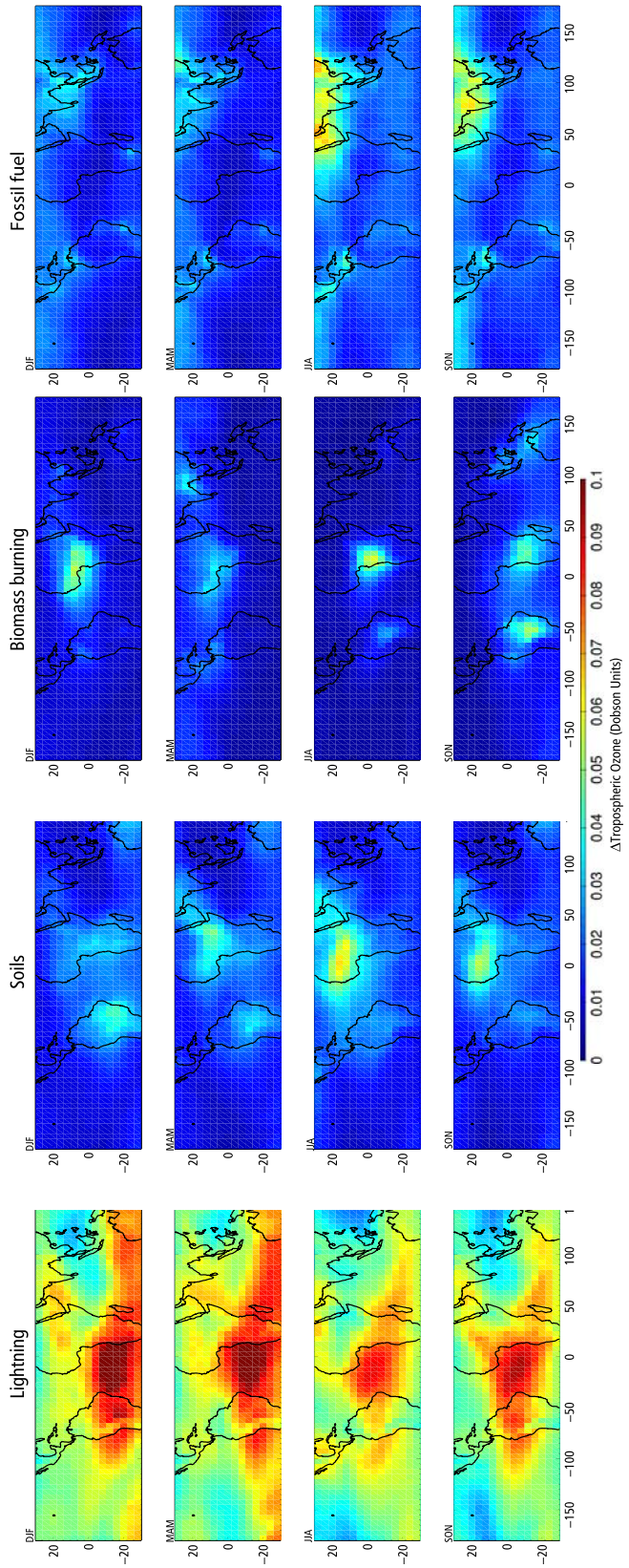

Figure 2. Calculated seasonal sensitivity of the tropospheric ozone column to the NO_x source, as determined by decreasing each source by 1%. The tropospheric ozone column differences (DU) between standard and sensitivity simulations are represented for lightning, soils, biomass burning, and fossil fuel combustion.

Table 1. Source Contribution to the South Atlantic Ozone Burden (Tg O_3)[a]

Season	Total[b]	Light. NO_x	Soil NO_x	Biomass burning NO_x	Fossil fuel NO_x	STE O_3	Background[c]	Afr. NO_x	S. Am. NO_x	East NO_x
DJF	8.87	3.48[d] (0.025)[e]	0.67 (0.007)	0.81 (0.004)	0.38 (0.004)	0.39	2.26	3.00 (0.017)	1.66 (0.013)	0.79 (0.006)
MAM	7.73	3.57 (0.022)	0.67 (0.006)	0.53 (0.008)	0.31 (0.004)	0.22	1.65	2.83 (0.012)	1.26 (0.009)	0.66 (0.005)
JJA	8.93	2.74 (0.017)	0.69 (0.005)	0.78 (0.005)	0.80 (0.003)	0.47	3.00	2.67 (0.008)	1.28 (0.008)	1.40 (0.010)
SON	9.32	2.90 (0.019)	0.57 (0.003)	1.05 (0.008)	0.70 (0.003)	0.58	3.06	2.63 (0.010)	2.12 (0.011)	1.10 (0.008)
Annual	8.71	3.17 (0.021)	0.62 (0.006)	0.79 (0.005)	0.60 (0.003)	0.42	2.50	2.80 (0.012)	1.60 (0.010)	0.98 (0.007)

[a]Sources and regions do not sum to 100% due to chemical nonlinearity.
[b]The South Atlantic is defined over 35°W-10°E/24°S-0°.
[c]The ozone background is calculated here using a simulation that excludes all tropical NO_x emissions.
[d]Values represent total contribution determined by difference with sensitivity simulation that excludes that source.
[e]Values in parenthesis indicate the sensitivity to a 1% perturbation.

NO_x sources: lightning, biomass burning, soils, and fossil fuel combustion to assess their relative contribution. In order to investigate the stratospheric contribution on tropical tropospheric ozone, we use a tagged ozone tracer to follow the stratospheric ozone flux across the tropopause as described by *Fiore et al.* [2002]. The tagged simulation subjects ozone produced in different regions of the atmosphere to archived three-dimensional fields of production and loss frequencies, allowing tropospheric ozone to be deconstructed into components from stratosphere and troposphere. When discussing the dynamical influence (section 3.2), we also comment on the regime south of 24°S. We conduct simulations for the year 2000 following a spin-up of 6 months.

3. Tropical Tropospheric Ozone

[14] In the following section, we decrease NO_x emissions by 1% to examine the sensitivity of O_3 to perturbations that may result from anthropogenic and natural activity or an altered climate. This small perturbation is designed to account for nonlinear O_3 chemistry especially in the lower troposphere. *Kunhikrishnan and Lawrence* [2004] find that nonlinearity associated with changes in photochemical regime becomes important for perturbations larger than 20–30%. For comparison and to approximate the role of each source, we also perform sensitivity studies by completely excluding a specific NO_x source (−100%). Since ozone production increases with NO_x more rapidly at low concentrations of NO_x [*Liu et al.*, 1987], both approaches will underestimate the true source contribution. Values will be preceded by ">" to emphasize this nonlinearity. For ease of comparison to the tropospheric ozone column (TOC) and the O_3 burden, we present the absolute difference between the standard simulation and the simulation with 100% reduction, followed in parenthesis by the results from the 1% perturbation. We also determine an O_3 background to estimate the enhancement for each source. It is quite challenging to estimate an O_3 background due to ambiguity in definition. As our study is based on O_3 sensitivity to NO_x emissions, we determine the O_3 background by excluding all NO_x sources over the tropics.

3.1. The Tropics and the South Atlantic

[15] Figure 1 shows seasonal tropospheric O_3 columns from two satellite instruments (GOME: left panels; OMI: right panels) that we interpret here with GEOS-Chem simulations (middle panels). The three data sets exhibit similar features despite OMI/MLS data being for a different year. The GEOS-Chem simulation well represents GOME ($r^2 > 0.9$, bias = 1.5 DU) and OMI/MLS ($r^2 > 0.8$, bias = 0.6 DU) on annual average over the tropics. The O_3 minimum over the Pacific is related to frequent convection of depleted O_3 associated with convection [*Folkins et al.*, 2002] and the Walker circulation [*Krishnamurti et al.*, 1993]. Persistent enhanced TOC are observed over the Atlantic in 2000 by GOME and in 2004 by OMI/MLS. The simulated ozone burden over the Atlantic is 10 Tg on annual average, with a maximum of 10.7 Tg in September–November (SON), during the maximum intensity of the zonal wave-one.

3.1.1. Sensitivity to Sources

[16] Figure 2 shows the seasonal sensitivity of tropospheric O_3 columns to NO_x emissions from either lightning, biomass burning, soils or fossil fuel combustion as determined from the difference between the standard simulation and a sensitivity simulation with 1% reduction. Table 1 contains the influence of the different NO_x sources on the O_3 burden calculated over the South Atlantic region. Lightning has the largest influence on tropical tropospheric ozone, accounting for >7.7 DU (0.056 DU) on annual average over the tropics and accounting for >37% of the annual average O_3 burden over the South Atlantic. Lightning has a large influence over a broad area [*Lamarque et al.*, 1996], affecting O_3 production far downwind of emissions [*Jacob et al.*, 1996]. As a result the spatial variation of the lightning influence on O_3 is significantly correlated with the tropical TOC (r^2 = 0.93). For comparison this corrleation is much lower globally (r^2 < 0.45). The similarity is also apparent between tropical TOC (Figure 1) and the lightning influence on tropical TOC (Figure 2). The maximum lightning influence is found largely in the Southern Hemisphere (Figure 2) where the persistent zonal wave-one pattern is apparent in the three data sets (Figure 1). The minimum influence is found over the northern Pacific Ocean, where the TOC is less than 25 DU. Lightning emissions are clearly the dominant source driving the zonal wave-one. For instance lightning accounts for 12.8 DU of the South Atlantic maximum on annual average, similar to the study of *Martin et al.* [2002]. The seasonal influence of lightning is maximum in DJF-MAM with >8.3 DU (0.06 DU), reflecting higher lightning activity and weaker biomass burning emissions. Lightning explains >39% of the South Atlantic O_3 burden in DJF, versus >30% in JJA.

[17] The contributions of biomass burning, fossil fuel combustion, and soil NO_x emissions to the TOC are, respectively, 6, 5, and 4 times smaller (with the 1% sensitivity approach) than that from lightning. The contribution from

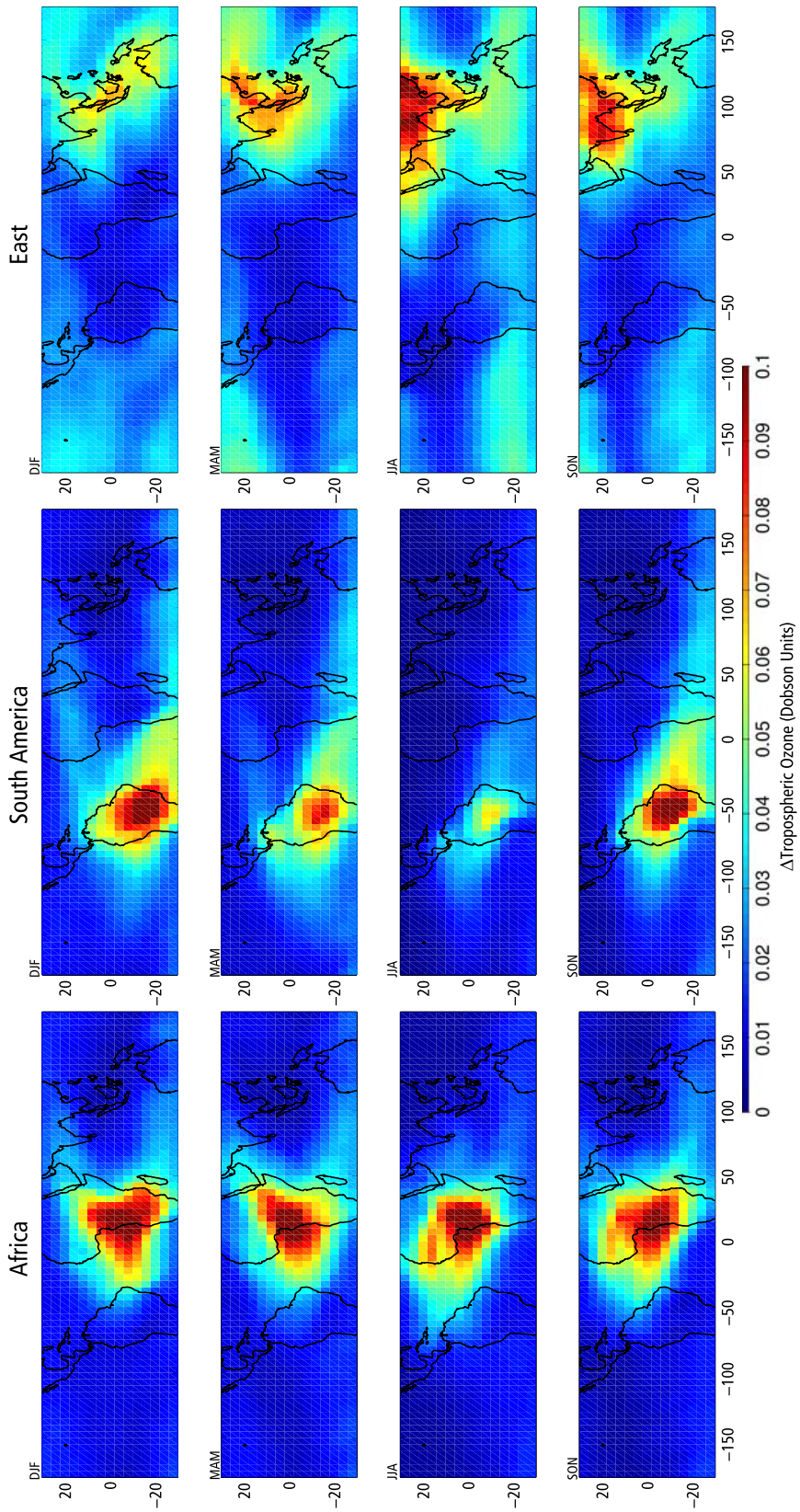

Figure 3. Seasonal sensitivity of the tropospheric ozone column to NO_x source, by decreasing each source by 1%. The tropospheric ozone column difference (DU) between the standard and sensitivity simulation is represented for (left) African sources, (middle) South American sources, and (right) eastern sources. Eastern sources are for India, South East Asia, and Oceania.

any of these sources does not exceed 2 DU (0.015 DU). A similarly weak influence is observed for the South Atlantic O_3 burden, with source sensitivity smaller than for lightning by factors of 4 for biomass burning and for soils, and 7 for fossil fuel (with 1% sensitivity approach). The weak effect of fossil fuel emissions reflects few sources in the surrounding area. The influence of surface sources is primarily close to emissions, and therefore has the largest influence on Africa.

[18] Soils exert considerable influence on TOC over Africa, with maximum effect during JJA through rain-induced emissions during the monsoon, as expected from the analysis of GOME NO_2 columns by *Jaeglé et al.* [2005]. Soil emissions in June are responsible for >8–10 DU (0.06–0.1 DU) over west equatorial Africa (17°W–35°E; 5°–10°N). Some influence of soil emissions on TOC is also found during rainy season over Brazil, during DJF with >2 DU (0.019 DU). Soil NO_x emissions have little seasonal variation in ozone over the South Atlantic.

[19] The contribution of biomass burning emissions to TOC is closely related to satellite observations of fires from the Along-Track Scanning Radiometer [*Arino et al.*, 2005] ($r^2 > 0.7$) reflecting the local effect of this source [*Valks et al.*, 2003]. The influence on O_3 is primarily in the burning hemisphere, in the Northern Hemisphere in DJF-MAM with >2.1 DU (0.010–0.015 DU), and the southern one in JJA-SON. This influence is predominantly on lower tropospheric O_3 [*Sauvage et al.*, 2005]. Over the South Atlantic, biomass-burning emissions have a maximum influence of 11% during SON, and minimum of 7% during MAM. Biomass burning exhibits a pronounced nonlinearity due to its concentrated emissions, with a weaker influence than soils in case of a small perturbation.

[20] Fossil fuel combustion primarily affects the eastern tropics. Weaker sources are present over Africa and South America, except for particular sites (Rio de Janeiro, Sao Paolo, Gauteng Province).

[21] The influence of stratospheric O_3 on tropical TOC, as calculated from the ozone flux across the tropopause in the tagged ozone simulation, is 1 DU on annual average only half the magnitude of either soils or biomass burning. During DJF and MAM, most of the stratospheric source is over the north Atlantic and Africa, as noted by *Cammas et al.* [1998], in relation with the seasonal variability of the subtropical jet. In JJA most of the stratospheric contribution is in the Southern Hemisphere. Over the South Atlantic, the stratospheric source is negligible, contributing to 5% of the ozone burden on annual average.

[22] In the absence of all tropical NO_x sources, an O_3 background of 28% remains, reflecting transport and chemical production from extratropical sources. The sum of O_3 produced from all NO_x sources, stratosphere-troposphere exchange and the O_3 background explains only 90% of the ozone burden because of ozone production nonlinearity. However, the seasonal influence and strength of the different sources is mostly independent of the O_3 chemistry nonlinearity (except for surface sources).

3.1.2. Sensitivity to Regions

[23] Numerous studies have investigated the influence on ozone over the South Atlantic from regional emissions from Africa [*Jonquières et al.*, 1998; *Krishnamurti et al.*, 1996; *Meyer-Arnek et al.*, 2005; *Edwards et al.*, 2003], from South America [*Pickering et al.*, 1996; *Jonquières and Marenco*, 1998; *Andreae et al.*, 2001], from India [*Lelieveld et al.*, 2001] and how they can be redistributed over the Atlantic [*Singh et al.*, 1996; *Thompson et al.*, 1996; *Chatfield et al.*, 2004]. In the following we investigate in a consistent fashion the role of regional emissions and transport on ozone in the tropics and particularly the Atlantic.

[24] Figure 3 shows seasonal influences on tropical TOC from total African, South American, and Eastern (India, South-East Asia, Australia) emissions. These regions account, respectively, for 7.3 Tg N/yr (42%), 4.4 Tg N/yr (25%), and 5.5 Tg N/yr (33%) of tropical NO_x sources. All the regions and associated sources exhibit primarily local influence, close to the region where they are emitted. As a result, the South Atlantic O_3 maximum is influenced more by adjacent continents than by long range transport.

[25] Eastern sources exert the largest influence on tropical TOC, with >7 DU (0.025 DU) annual average, reflecting the divergent circulation. The maximum local effect is found during JJA and SON (>6.8 DU), but also on a broader area than sources situated over Africa and South America. Indeed, there is influence throughout the Pacific and Indian Oceans, in JJA and SON. Eastern emissions generally have little influence on the African continent. However, in Figure 3 a particularly large influence upon North Africa, close to Egypt, occurs through long-range transport in JJA, with >6 DU (0.037 DU). The upper level anticyclone associated with the Indian monsoon [*Hoskins and Rodwell*, 1995; *Rodwell and Hoskins*, 2001] merged with the Tropical Easterly Jet, has maximum amplitude during JJA [*Hastenrath*, 1985] and allows advection of Eastern source emissions to North Africa and the Atlantic. Eastern sources account for >11% of the South Atlantic ozone burden, with a maximum influence in JJA. Convective outflow is advected to the northern part of South Atlantic, where Hadley cells can ensure southernward and slow redistribution.

[26] Sources situated over Africa and South America exhibit maximum influence on the regional TOC. African sources account for >5 DU (0.020 DU) and South America for >4 DU (0.018 DU) of the entire tropical troposphere, on annual average, driven by the higher emissions over the African continent. Both regions have high influence in DJF when there is substantial lightning activity over South America, as well as lightning and biomass burning [*Marufu et al.*, 2000] over Africa. Africa, north of the equator, is the region most influenced by African sources, with >10 DU (0.061 DU) on annual average, versus >8 DU (0.057 DU) for Southern Africa. These regional sources account for most of the South Atlantic ozone burden. African emissions are responsible for >30% of the South Atlantic ozone burden, and South American emissions for >18% on annual average. These regions have more similar influence on the South Atlantic ozone burden with the 1% sensitivity simulation. African emissions have a greater effect in DJF with a contribution of more than 33%, largely due to lightning rather than north African biomass burning emissions. Similar conclusions can be made for the maximum influence of South America in SON of >22%, due to substantial lightning activity.

[27] The seasonal maximum of the zonal wave-one in SON reflects the confluence of both South American and African sources, with >22 and >28%, respectively, as well as long-range transport from eastern sources contributing >11% of the burden. In contrast, during the MAM minimum

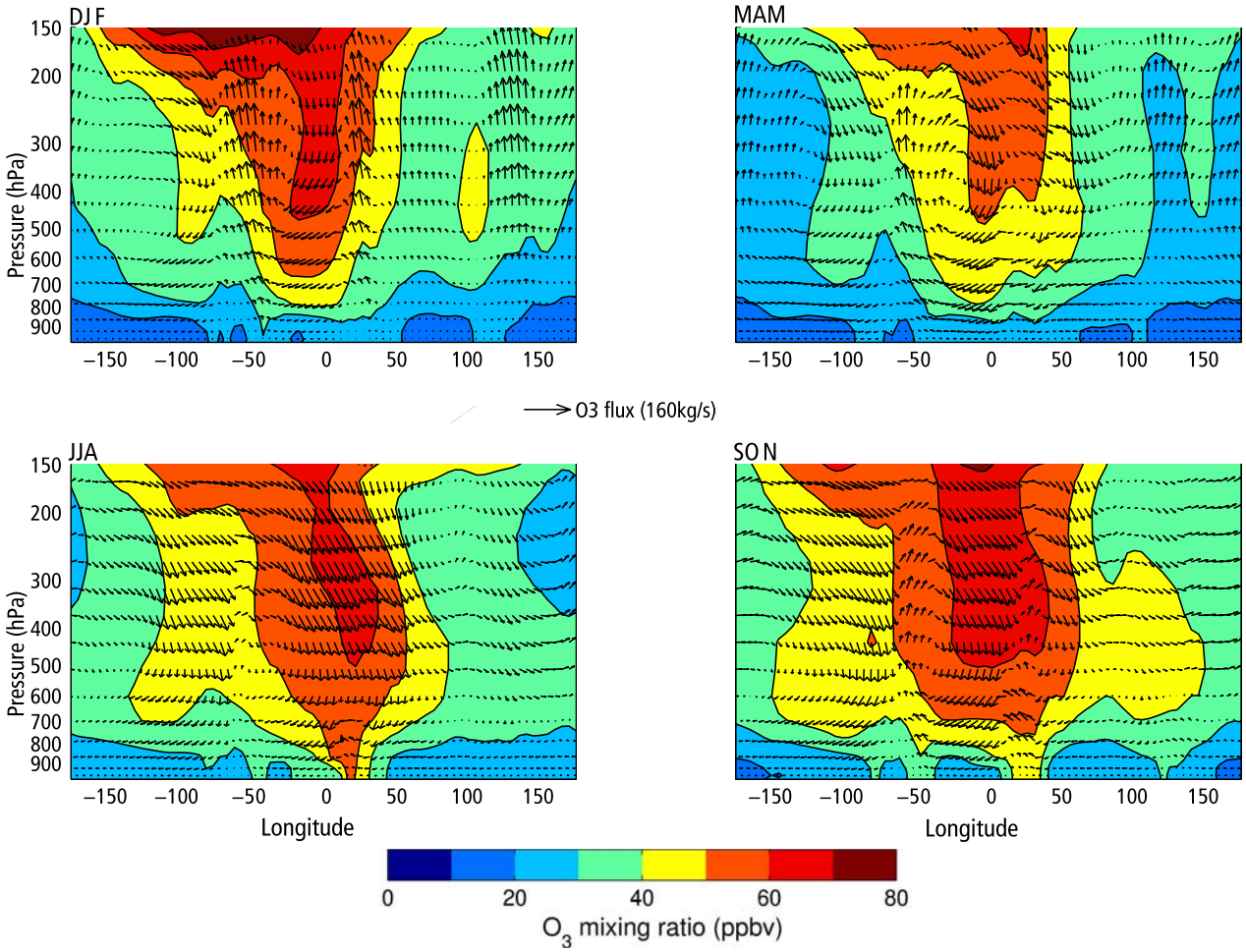

Figure 4. Vertical cross-section of the seasonal O_3 mixing ratios (ppbv) averaged over latitude, between 24°S and 0°. Arrows represents the zonal and vertical components of the O_3 flux in the cross section. The ozone flux is calculated for each grid point using the vertical and horizontal wind components. The vertical component has been scaled by a factor of 8 for better visibility.

of O_3 over the South Atlantic, Africa has a maximum influence, whereas South America and the East have minimum influence.

3.2. Dynamical Processes Affecting the Atlantic Ozone Maximum

[28] Lightning is the dominant "fuel" of the zonal wave-one with a maximum influence on O_3 over the South Atlantic as discussed in section 3.1, and apparent from Figures 1 and 2. It is noteworthy that lightning is absent over this region of the South Atlantic Anticyclone. This region exhibits persistent convergence and subsidence, allowing O_3 production and accumulation during downward transport [*Newell*, 1979; *Krishnamurti et al.*, 1993; *Jacob et al.*, 1996; *Moxim and Levy*, 2000; *Wang et al.*, 2006]. The subtropical South Atlantic high, a quasi stationary anticyclone [*Hastenrath*, 1985], and energy balance drive the radiative subsidence over that region, through convergent flow at higher altitude, representing the "engine" of O_3 buildup over the South Atlantic. However, different flow regimes occur close to the equator and near the subtropics. For that reason in this section we also discuss the extratropical southern Atlantic (32°S–24°S).

[29] Figure 4 provides insight into the processes affecting the southern tropics and the South Atlantic O_3 maximum in particular. It shows the simulated zonal cross-section of the seasonal O_3 mixing ratio between 0° and 24°S. This simulation reproduces the year-round zonal wave-one pattern centered near 40°E–60°W, with maximum amplitude in SON and minimum in MAM, as inferred from in situ measurements [*Thompson et al.*, 2003; *Sauvage et al.*, 2006, 2007] and SAGE II data [*Wang et al.*, 2006]. The extension of the wave one into the lower troposphere resulted from the improved African emissions calculated from satellite observations as implemented by *Sauvage et al.* [2007]. In contrast, the southern subtropics (not shown) exhibit a very weak wave one pattern.

[30] The ozone fluxes in Figure 4 clearly show the strong subsident feature of the O_3 flux for all seasons over the South Atlantic, allowing downwelling of air masses loaded with enhanced O_3 and its precursors. It supports the previous discussion of a preponderance of regional processes in controlling the O_3 column enhancement. The O_3 maximum is bounded by deep convection as illustrated by O_3 fluxes above South America (70°–35°W) and above Africa (20°–40°E). Over those regions the O_3 concentration is

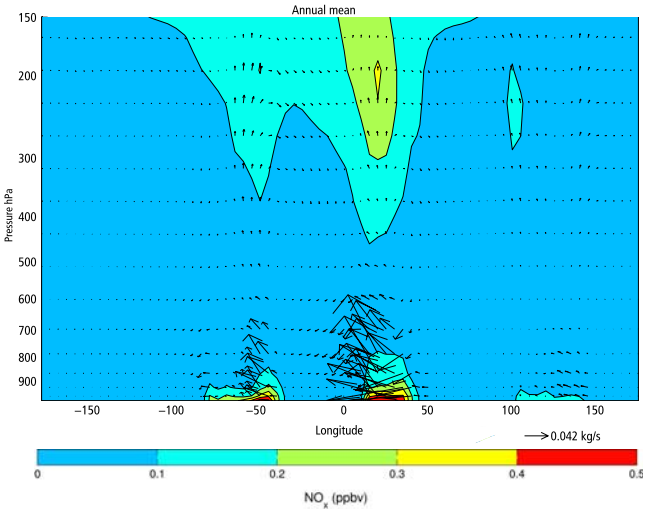

Figure 5. Vertical cross-section of the annual NO_x mixing ratios (ppbv) averaged over latitude, between 24°S and 0°. Arrows represent the zonal and vertical components of the NO_x flux in the cross section. The vertical component has been scaled by a factor of 8 for clarity.

lower than in the maximum of the zonal wave-one, and with strong vertical O_3 gradient. In the southern subtropics, subsidence is weak over the South Atlantic as this region is on the southern edge of the convergence area of the South Atlantic high. Our simulation of background O_3 exhibits a wave one pattern, in agreement with the passive tracer experiment of *Krishnamurti et al.* [1996]. However, the wave one pattern depicted with the simulation of background O_3 exhibits considerably weaker O_3 burden, indicating that the photochemical production is responsible for its magnitude as discussed below.

[31] Figure 5 shows annual mean NO_x fluxes. As described by *Jacob et al.* [1996], deep convection over continents injects NO_x from surface sources and lightning into the upper troposphere, driving O_3 production. The uplift of surface sources also exists in the subtropics (not shown), with weaker lightning influence compared to the tropics. O_3 increases during upper tropospheric zonal advection and descent over oceans. Destruction in the lower troposphere occurs with high humidity and low NO_x concentrations. Figures 4 and 5 confirm this scheme, highlighting the regional convection over continents, the zonal advection as part of Walker circulation, and the radiative subsidence over the South Atlantic anticyclone area, as major contributors to the O_3 enhancement.

[32] Table 2 quantifies the regional O_3 budget over the tropical South Atlantic. Chemical production and loss are the dominant terms, reflecting the convective injection of NO_x into the free troposphere.

[33] Table 3 contains the seasonal contribution of each source to the NO_x burden over the tropical South Atlantic. Lightning is responsible for more NO_x in the tropical South Atlantic when the ITCZ is further south, during DJF-MAM, with 35 pptv influence. Lightning supplies 59% of the NO_x in the tropical South Atlantic, nearly three times more than all surface sources combined. For comparison, *Moxim and Levy* [2000] found 49% of tropospheric NO_x transported into that region comes from lightning. Our higher lightning source, (6 Tg N/yr versus 4 Tg N/yr), is part of that difference. It is interesting that in the subtropical part of the Atlantic where a very weak wave one pattern is found, lightning and total surface sources make similar contributions to NO_x (28 and 23 pptv, respectively).

[34] Figure 6 shows the annual (top) and seasonal (bottom, SON) tropical O_3 mixing ratio attributed to lightning, and to all surface sources. Lightning has the largest influence on the southern tropics. A particularly large lightning contribution to the O_3 mixing ratio appears at the top of the ascending branches (near 150–200 hPa) and in the middle and upper troposphere of the tropical Atlantic downwind of lighting emissions. The maximum influence of surface sources on O_3 appears in the lower troposphere above continents, mostly when biomass burning is active. The role of surface sources in the O_3 enhancement is much less than lightning and exhibits more seasonal variation. In the southern subtropics lightning still has the largest influence, but is somewhat weaker.

[35] Figure 7 highlights zonal transport through a meridional-vertical cross-section averaged over 35°W–10°E where the overturning of the Hadley cells is clearly visible. Strong convection occurs over northern Africa (5°N–10°N) injecting NO_x into the upper troposphere. This is followed by slow

Table 2. Tropospheric Ozone Budget of the South Atlantic[a]

O_3 budget parameters	Values, Tg O_3 yr^{-1}
Chemical Production[b]	151
Chemical Loss[b]	160
Deposition	6
Upward Influx	−15
Net Zonal Flux[c]	−24
Net Meridional Flux[d]	9

[a]The tropical South Atlantic is defined over 35°W-10°E/24°S-0°, from the surface to the tropopause.

[b]The chemical production and loss are calculated for odd oxygen family with $O_x = O_3 + O + NO_2 + 2NO_3 + PANs + HNO_3 + HNO_4$, to avoid accounting for rapid cycling of ozone with short-lived species that have little implication in the budget.

[c]The net zonal flux is calculated as the difference of the integrated flux for the eastern and the western edges of the South Atlantic.

[d]The net meridional flux is calculated as the difference of the integrated flux for the northern and the southern edges of the South Atlantic.

Table 3. Tropical Tropospheric OH and Tropical South Atlantic Tropospheric NO_x, and the Contribution From the Different Sources

	NO_x (pptv)		
Season	NO_x	$NO_{x\ light}$	$NO_{x\ surf}$
DJF	58	36	9
MAM	50	34	6
JJA	52	27	13
SON	56	30	13
ANNUAL	54	32	11

	OH (10^6 molec cm^{-3} s^{-1})		
Season	OH	OH_{light}	OH_{surf}
DJF	1.52	0.62	0.36
MAM	1.54	0.63	0.32
JJA	1.46	0.57	0.41
SON	1.55	0.55	0.50
ANNUAL	1.51	0.59	0.40

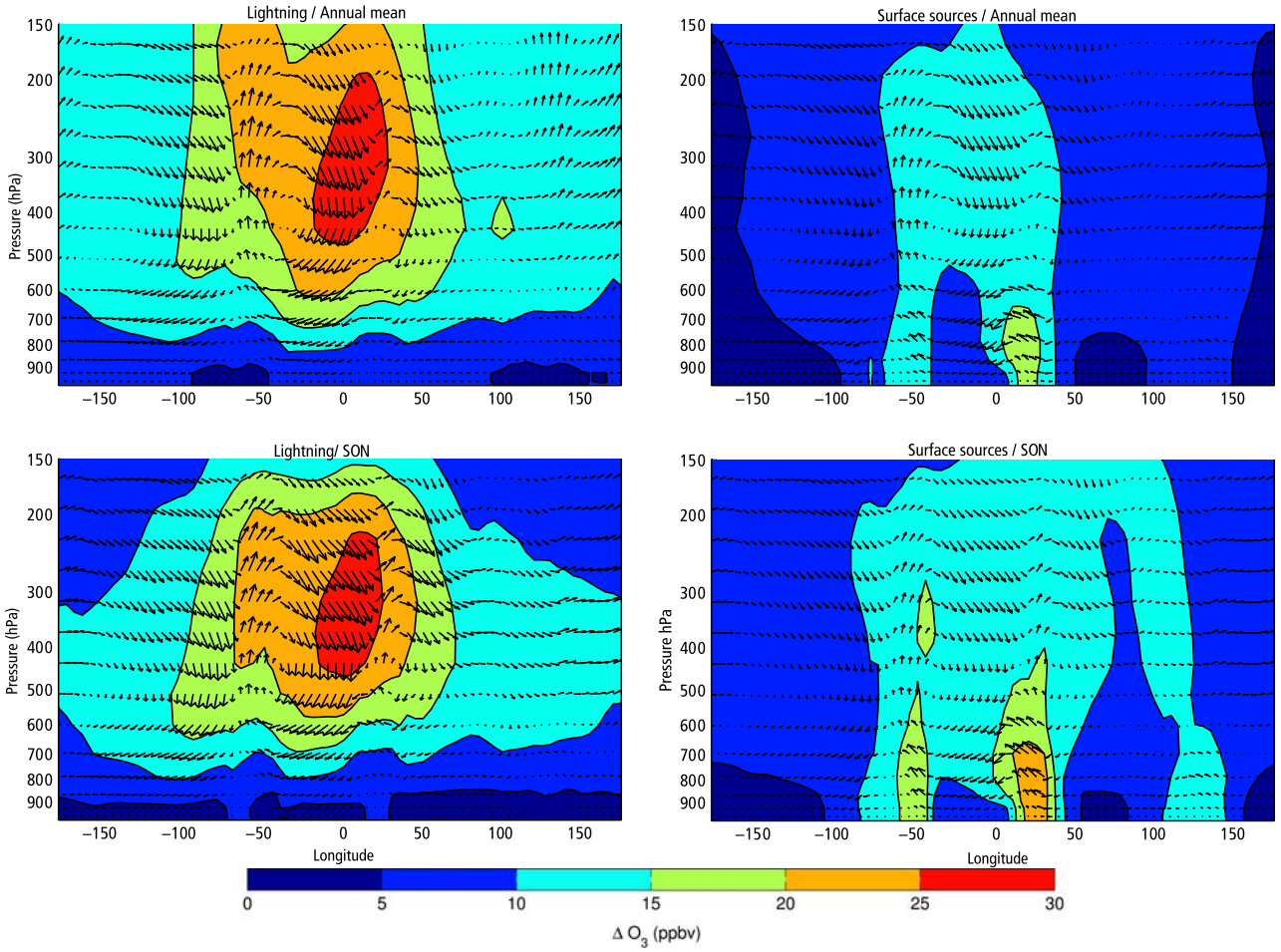

Figure 6. Vertical cross-section of the contribution of lightning (left), and surface sources (right), to the O_3 mixing ratios (ppbv) averaged over latitude, between 24°S and 0°. Arrows represent the meridional and vertical components of the source contribution to the O_3 flux. Top panels are annual mean and bottom panels are for SON.

poleward transport and strong subsidence over the South Atlantic. In contrast, to the North Atlantic, the South Atlantic can be supplied by surface sources in DJF (not shown) through a similar circulation depicted in Figure 7, confirming conclusions of *Chatfield et al.* [2004] and *Sauvage et al.* [2006] for the remaining O_3 paradox over the Atlantic. During DJF and SON the position of the ITCZ facilitates efficient redistribution of fire products into the southern middle troposphere.

[36] To summarize the South Atlantic O_3 maximum is driven by persistent radiative subsidence over the South Atlantic anticyclone area, sustained by injection of NO_x by deep convection over South America and Africa. O_3 is produced during transport converging into that area in both meridional and zonal transport pathways. If various sources play the role of "fuel" for this dynamical and photochemical "engine", lightning emissions are the most important source.

[37] In the next section we examine why lightning has the most influence despite a source strength similar to biomass burning or soils.

3.3. Ozone Production Efficiency Over the Tropics

[38] The ozone production efficiency (OPE), the number of O_3 molecules produced per NO_x molecule consumed [*Liu*

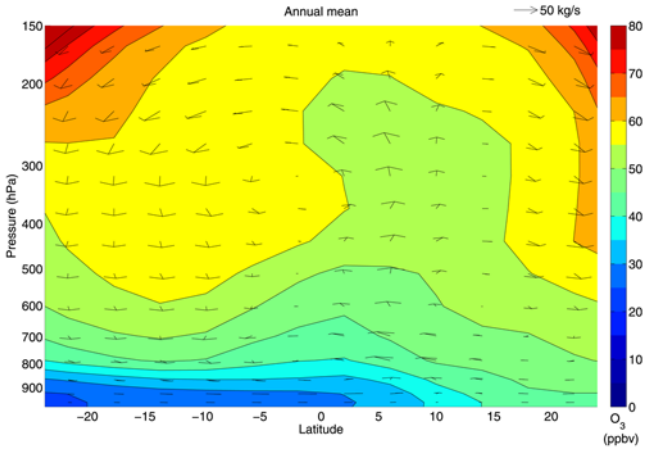

Figure 7. Vertical cross-section of the annual O_3 mixing ratios (ppbv) averaged over longitude, between 35°W and 10°E. Arrows represents the meridional and vertical components of the O_3 flux in the cross section. The vertical component has been scaled by a factor of 8 for visibility.

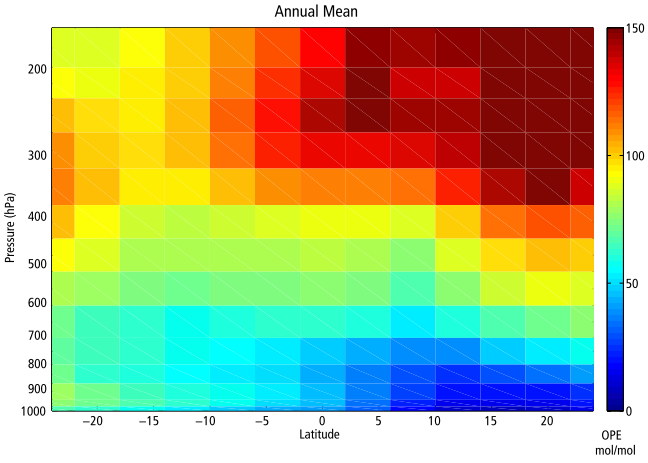

Figure 8. Annual mean Ozone Production Efficiency (OPE) represented in meridional (24°S–24°N) cross-section over the South Atlantic O_3 maximum between 35°W and 10°E.

et al., 1987], provides a useful metric to understand tropical tropospheric O_3. We calculate OPE in the model using HNO_3 production as a proxy for NO_x loss. The OPE provides a measure of the nonlinear dependence of net O_3 production on NO_x.

[39] Figure 8 shows the OPE along vertical cross-sections annually averaged over the tropical South Atlantic O_3 maximum meridional band (35°W–10°E). OPE generally increases with altitude due to intense radiation, low humidity, and relatively low NO_x concentrations. In the middle and upper troposphere the OPE is maximum, from 100 to more than 150 mol/mol. The upper tropospheric OPE minimum follows the ITCZ where humidity and NO_x concentrations are higher. At these altitudes the seasonal OPE (not shown) is much higher in the opposite hemisphere of convection. However, there is persistent high OPE in the tropical South Atlantic region with 98 mol/mol on annual average. As a result O_3 chemical production dominates the O_3 source of the South Atlantic (Table 2). Particularly low OPE appears in the lower troposphere north of 5°N during DJF and MAM because of the high NO_x concentrations from biomass burning over West Equatorial Africa.

[40] We assess the OPE of the different sources by archiving the production of O_x (PO_x) and HNO_3 ($PHNO_3$) in sensitivity simulations with perturbations to each source:

$$\mathrm{OPE}_{\mathrm{source}} = \frac{(\mathrm{PO}_x)_{\mathrm{standard}} - (\mathrm{PO}_x)_{\Delta_{\mathrm{source}}}}{(\mathrm{PHNO}_3)_{\mathrm{standard}} - (\mathrm{PHNO}_3)_{\Delta_{\mathrm{source}}}}$$

Results are depicted in Table 4. Due to chemical nonlinearity, the results from this approach can not be directly related to the OPE of 98 mol/mol presented above. Therefore we calculate an OPE for all sources with a sensitivity simulation in which all NO_x sources are reduced by 1%. Then resulting OPE of 12 mol/mol can be directly compared to the individual sources that follow.

[41] Lightning exhibits the highest OPE, 32 mol/mol on annual average, versus 14 mol/mol for biogenic soil emissions, 10 mol/mol for biomass burning and 13 mol/mol for fossil fuel emissions. Soils and fossil fuels have nearly constant OPE. In contrast, biomass burning has stronger seasonal variation of OPE. The diffuse nature of lightning NO_x emissions and direct emission into the middle and upper troposphere explains its high OPE.

3.4. Oxidizing Capacity of the Tropical Troposphere

[42] Table 3 contains the seasonal mean of tropical tropospheric OH concentrations, and the component of OH concentrations attributable to each NO_x source, as determined by difference between the standard simulation and simulations without a specific source. Our simulated tropical mean OH is 6% higher than that inferred from measurements of related species by *Spivakovsky et al.* [2000]. OH is highly sensitive to lightning NO_x, as noted by *Labrador et al.* [2004] in a global analysis. Indeed, this source contributes to >39% of the 1.5×10^6 molec cm^{-3} simulated over the tropics on annual average. Other NO_x sources account for substantially less OH, >8% for soils, >7% for biomass burning, and >11% for fossil fuel. The sensitivity simulations with a 1% perturbation reveal that the lightning contribution is three times higher than that from soils or fossil fuel, and five times higher than that from biomass burning.

[43] Lightning is the primary NO_x source determining the oxidation capacity of the troposphere. Future change in the lightning source would have considerable implications for atmospheric oxidation. Indeed, some studies predict an increase in lightning intensity in an altered climate [*Price and Rind*, 1994; *Hauglustaine et al.*, 2005]. Lightning has similar influence on both tropical tropospheric O_3 and OH concentrations. In the upper troposphere high NO and O_3 concentrations related to lightning emission appear, allowing greater production of OH through photolysis of O_3 and, as noted by *Labrador et al.* [2004], through reaction of NO with HO_2.

4. Error Estimates: Sensitivity Studies

[44] In the following we estimate the error of our O_3 budget analysis over the tropics and the South Atlantic, by focusing on the largest uncertainties.

4.1. Lightning Emissions

[45] Recent comparison of GEOS-Chem simulations with in situ and satellite observations yields upper and lower bounds for the lightning source of 8 and 4 Tg N/yr [*Martin et al.*, 2007; *Sauvage et al.*, 2007]. The resultant uncertainty in both the simulation of the South Atlantic O_3 burden and OH is 10%. Even for the lower limit of 4 Tg N/yr, lightning remains the main NO_x source driving the tropical O_3 burden, the South Atlantic maximum, and atmospheric oxidation.

Table 4. Average Tropical Tropospheric OPE (mol mol^{-1}) and for Different Sources ($OPE\Delta_{source}$)

Ozone Production Efficiency	Value, mol mol^{-1}
OPE	98
$OPE\Delta_{all}$[a]	12
$OPE\Delta_{light}$	32
OPE Δ_{soils}	14
$OPE\Delta_{bb}$	10
$OPE\Delta_{fossil\ fuel}$	13

[a] $OPE\Delta_{all}$ is calculated by perturbing all NOx sources by 1%.

[46] Another uncertainty arises from the vertical distribution of lightning emissions. Recent studies provide evidence that the NO_x production efficiency of intracloud (IC) flashes could be the same order of magnitude as cloud to ground (CG) flashes [*DeCaria et al.*, 2000; *Fehr et al.*, 2004]. A sensitivity study using an IC/CG ratio of 0.7 instead of 0.1 increases the ozone burden by 3.5% (0.32 Tg) on annual average. The influence on OH concentrations is negligible, around 2%.

4.2. Dynamics

[47] We also examined the sensitivity of our results to a different dynamical scheme (GEOS-3). The resultant annual mean O_3 burden over the South Atlantic decreases by 4%, with a corresponding decrease in tropical mean OH of 14%.

[48] There are three primary differences between GEOS-3 and GEOS-4. The cloud optical depth is higher in GEOS-3 than in GEOS-4 [*Liu et al.*, 2006; *Wu et al.*, 2007], reducing photolysis frequencies in GEOS-3. The GEOS-3 convective parameterization has a weaker deep outflow mode [*Folkins et al.*, 2006] and a higher altitude of convective detrainment. These differences yield O_3 variation of 10–20% in the middle and upper troposphere [*Sauvage et al.*, 2007] and a 10% variation on the production of O_x [*Wu et al.*, 2007]. Cloud radiative properties and convective transport are the major sources of uncertainty in the oxidizing capacity of the tropical troposphere.

4.3. Surface Sources

[49] Here we assess how uncertainties in surface sources and heterogeneous processes affect the O_3 budget over the Atlantic. As discussed in section 2, *Sauvage et al.* [2007] applied GOME observations of tropospheric NO_2 columns to provide top-down constraints on soils and biomass burning NO_x emissions, increasing global NO_x emissions by 2.6 Tg N/yr for soils and 1.1 Tg N/yr for biomass burning. As a result the South Atlantic O_3 burden increased by only 3%. According to *Holland et al.* [1999] NO_x sources are within 3–13 Tg N/yr for biomass burning and 1–21 Tg N/yr for soils. Even for emissions at the upper limit for both surface sources, and using the lower limit for lightning, lightning remains the major contributor to the South Atlantic O_3 burden and OH.

[50] We conduct a sensitivity simulation with the MEGAN inventory [*Guenther et al.*, 2006] to assess the error estimated on the contribution of biogenic volatile organic compounds. Isoprene emissions increase by 50%, to 600 Tg C/yr. However, the influence on the ozone burden of the South Atlantic maximum is negligible (±1.5%). Varying VOC emissions from biomass burning by a factor of 8 is also negligible, introducing a ±2% change in the South Atlantic O_3 burden.

4.4. Heterogeneous Chemistry

[51] Uncertainty in heterogeneous processes also has little effect on the tropical Atlantic O_3 burden. The two most uncertain processes examined here are uptake of HO_2 and HNO_3. Removing these processes changes the South Atlantic ozone burden by ±2.5%.

4.5. Stratospheric Flux

[52] Upper and lower limits on the stratospheric O_3 flux are 680 Tg O_3/yr to 400 Tg O_3/yr [*Olsen et al.*, 2001; *Hauglustaine et al.*, 1998]. This implies difference in the O_3 burden over the tropical South Atlantic < ±6%.

5. Conclusions and Perspective

[53] In this study we used a state of the art global chemical transport model, using an emission inventory that was constrained with satellite observations and validated over the tropics [*Sauvage et al.*, 2007], to quantify the O_3 budget of the tropics and the South Atlantic ozone maximum. Sensitivity studies were conducted with perturbations on NO_x sources and regions, in which NO_x emissions were decreased by 1 and 100%. This approach allows assessment of ozone production nonlinearity on our conclusions.

[54] Lightning is the dominant contributor to tropical tropospheric ozone, accounting for more than 28% of the tropical tropospheric O_3 burden on annual average, as determined from a sensitivity simulation that excludes this source. The contributions from surface sources are smaller, with >7% for soils, >7% for biomass burning, and >8% for anthropogenic sources on annual average, despite similar source strengths. These values represent lower bounds due to O_3 production nonlinearity. However, the relative contribution of each source is largely independent of chemical nonlinearity, except for competition between surface sources. Stratosphere-troposphere exchange accounts for 5% of tropical tropospheric O_3. The O_3 background accounts for 30% of the tropical tropospheric O_3 burden in the absence of tropical NO_x sources, reflecting photochemical production and transport of NO_x and O_3 from outside the region.

[55] The greater contribution of lightning compared to other sources, despite similar strengths, is explained by the high ozone production efficiency (OPE) of the tropical upper troposphere. Lightning is emitted directly into the middle and upper troposphere, where low OH abundance and high NO/NO_2 ratios enhance OPE. The OPE of tropical lightning emissions (32 mol/mol) is twice that of any surface source.

[56] Lightning is the major contributor of the oxidizing capacity of the tropical troposphere, accounting for >39% of OH concentrations, much higher than all surface emissions combined (>26%). Future evolution of the oxidizing capacity of the atmosphere will be closely coupled to lightning intensity.

[57] Over the South Atlantic O_3 maximum, lightning NO_x accounts for >37% of the O_3 burden in annual average, against >7% for soil NO_x, >9% for biomass burning NO_x, and >5% for fossil fuel NO_x sources. Stratospheric O_3 has little role, 5%. An O_3 background of 28% remains in the absence of all tropical NO_x emissions.

[58] The South Atlantic maximum is driven by dynamical processes, with permanent radiative subsidence over the quasi-stationary South Atlantic anticyclone area. This area acts as a convergence zone of meridional and zonal fluxes. Chemical production and loss are the dominant terms.

[59] The main geographic contribution appears to be regional with the two bounded continents. Convection in the ITCZ over these adjacent continents, Africa and South America (with respective NO_x sources representing 30 and 18% of the South Atlantic ozone burden), allows uplifting of "fuel", i.e., O_3 precursors emitted by surface sources and most of all of lightning NO_x emissions. In the middle and

upper troposphere with low humidity rates and high UV radiation, O_3 can buildup and be pumped down by radiative subsidence, giving rise to the zonal wave-one pattern. Long-range transport has influence mostly in JJA, when the tropical easterly jet is maximum, accounting for 15% of the O_3 burden, against 11% on annual average.

[60] The maximum O_3 intensity over the South Atlantic in SON is explained by a combination of lightning and soil NO_x sources, but also a maximum intensity of fires over Africa and South America, as well as a maximum in long range transport.

[61] Despite nonlinearity in O_3 production, the previous statements are similar for 1 or 100% reduction of sources, in terms of seasonality and intensity. The primary difference comes in the relative contribution of soils versus biomass burning or fossil fuels, which is shifted depending of the configuration, and reflected in the regional contributions for South America and Africa.

[62] Finally, we assess uncertainties of our study by conducting sensitivity simulations of the lightning source strength, lightning vertical distribution, dynamical scheme, surface emissions, heterogeneous chemistry, and stratospheric flux. Uncertainty in the ozone burden over the Tropical Atlantic is driven by lightning emissions and dynamical fields (convective parameterization and clouds). Lightning and dynamical processes account for most of uncertainty in the oxidizing power of the tropical troposphere. These uncertainties do not change our primary conclusions, that lightning is the dominant NO_x source affecting the tropical O_3 burden.

[63] **Acknowledgments.** This work was supported by the Atmospheric Composition Program of NASA's Earth-Sun System Division. We thank anonymous reviewers for helpful comments that improved the manuscript.

References

Alexander, B. J., et al. (2005), Sulfate formation in sea-salt aerosols: Constraints from oxygen isotopes, *J. Geophys. Res.*, *110*, D10307, doi:10.1029/2004JD005659.

Andreae, M. O., et al. (2001), Transport of biomass burning smoke to the upper troposphere by deep convection in the equatorial region, *Geophys. Res. Lett.*, *28*(6), 951–954.

Arino, O., S. Plummer, and D. Defrenne (2005), Fire disturbance: The ten years time series of the ATSR world fire atlas, paper presented at *Proceedings of the MERIS-AATSR workshop*, Frascati, Italy, September 2005.

Bey, I., et al. (2001), Global modeling of tropospheric chemistry with assimilated meteorology: Model description and evaluation, *J. Geophys. Res.*, *106*, 23,073–23,096.

Bloss, W. J., M. J. Evans, J. D. Lee, R. Sommariva, D. E. Heard, and M. J. Pilling (2006), The oxidative capacity of the troposphere: Coupling of field measurements of OH and a global chemistry transport model, *Faraday Discuss.*, *130*, 425–436.

Burrows, J. P., et al. (1999), The Global Ozone Monitoring Experiment (GOME): Mission concept and first scientific results, *J. Atmos. Sci.*, *56*, 151–175.

Cammas, J.-P., S. Jakoby-Koaly, K. Suhre, R. Rosset, and A. Marenco (1998), The subtropical potential vorticity barrier as seen by MOZAIC flights, *J. Geophys. Res.*, *103*, 25,681–25,694.

Chatfield, R. B., H. Guan, A. M. Thompson, and J. C. Witte (2004), Convective lofting links Indian Ocean air pollution to paradoxical South Atlantic ozone maxima, *Geophys. Res. Lett.*, *31*, L06103, doi:10.1029/2003GL018866.

Christian, H. J., R. J. Blakeslee, D. J. Boccipio, W. L. Boeck, D. E. Buechler, K. T. Driscoll, S. J. Goodman, J. M. Hall, D. M. Mach, and M. F. Stewart (2003), Global frequency and distribution of lightning as observed from space by the optical transient detector, *J. Geophys. Res.*, *108*(D1), 4005, doi:10.1029/2002JD002347.

de F. Forster, P. M., and K. P. Shine (1997), Radiative forcing and temperature trends from stratospheric ozone changes, *J. Geophys. Res.*, *102*(D9), 10,841–10,856.

DeCaria, A. J., K. E. Pickering, G. L. Stenchikov, J. R. Scala, J. L. Stith, J. E. Dye, B. A. Ridley, and P. Laroche (2000), A cloud-scale model study of lightning-generated NO_x in an individual thunderstorm during STERAO-A, *J. Geophys. Res.*, *105*(D9), doi:10.1029/2000JD900033.

Edwards, D. P., et al. (2003), Tropospheric ozone over the tropical Atlantic: A satellite perspective, *J. Geophys. Res.*, *108*(D8), 4237, doi:10.1029/2002JD002927.

Evans, M. J., and D. J. Jacob (2005), Impact of new laboratory studies of N2O5 hydrolysis on global model budgets of tropospheric nitrogen oxides, ozone, and OH, *Geophys. Res. Lett.*, *32*, L09813, doi:10.1029/2005GL022469.

Fairlie, T. D., D. J. Jacob, and R. J. Park (2007), The impact of transpacific transport of mineral dust in the United States, *Atmos. Environ.*, in press.

Fehr, T., H. Hller, and H. Huntrieser (2004), Model study on production and transport of lightning-produced NO_x in a EULINOX supercell storm, *J. Geophys. Res.*, *109*, D09102, doi:10.1029/2003JD003935.

Fishman, J., C. E. Watson, J. C. Larsen, and J. A. Logan (1990), Distribution of tropospheric ozone determined from satellite data, *J. Geophys. Res.*, *95*(D4), 3599–33,617.

Fiore, A. M., D. J. Jacob, I. Bey, R. M. Yantosca, B. D. Field, A. C. Fusco, and J. G. Wilkinson (2002), Background ozone over the United States in summer: Origin, trend, and contribution to pollution episodes, *J. Geophys. Res.*, *107*(D15), 4275, doi:10.1029/2001JD000982.

Fiore, A. M., L. W. Horowitz, E. J. Dlugokencky, and J. J. West (2006), Impact of meteorology and emissions on methane trends, *Geophys. Res. Lett.*, *33*, L12809, doi:10.1029/2006GL026199.

Folkins, I., C. Braun, A. M. Thompson, and J. Witte (2002), Tropical ozone as an indicator of deep convection, *J. Geophys. Res.*, *107*(D13), 4184, doi:10.1029/2001JD001178.

Folkins, I., P. Bernath, C. Boone, A. Eldering, G. Lesins, R. V. Martin, B.-M. Sinnhuber, and K. Walker (2006), Testing convective parameterizations with tropical measurements of HNO_3, CO, H_2O, and O_3: implications for the water vapor budget, *J. Geophys. Res.*, *111*, D23304, doi:10.1029/2006JD007325.

Froidevaux, L., et al. (2007), Early validation analyses of atmospheric profiles from EOS MLS on the Aura satellite, *IEEE Trans. Geosci. Remote Sens.*, in press.

Guenther, A., T. Karl, P. Harley, C. Wiedinmyer, P. I. Palmer, and C. Geron (2006), Estimates of global terrestrial isoprene emissions using MEGAN (Model of Emissions of Gases and Aerosols from Nature), *Atmos. Chem. Phys. Disc.*, *6*, 107–173.

Hanisch, F., and J. N. Crowley (2003), Ozone decomposition on Saharan dust: an experimental investigation, *Atmos. Chem. Phys.*, *3*, 119–130.

Hastenrath, S. (1985), Climate and circulations of the tropics, Springer, New York.

Hauglustaine, D. A., G. P. Brasseur, S. Walters, P. J. Rasch, J.-F. Muller, L. H. Emmons, and M. A. Carroll (1998), MOZART, a global chemical transport model for ozone and related chemical tracers: 2. Model results and evaluation, *J. Geophys. Res.*, *103*(D21), 28,291–28,336.

Hauglustaine, D. A., J. Lathiere, S. Szopa, and G. A. Folberth (2005), Future tropospheric ozone simulated with a climate-chemistry-biosphere model, *Geophys. Res. Lett.*, *32*, L24807, doi:10.1029/2005GL024031.

Hoskins, B. J., and M. J. Rodwell (1995), A model of the Asian summer monsoon: Part I. The global scale, *J. Atmos. Sci.*, *52*(9), 1329–1340.

Holland, E. A., F. J. Dentener, B. H. Braswel, and J. M. Sulzman (1999), *Biogeochemistry*, *46*, 7–43.

Jacob, D. J., et al. (1996), Origin of ozone and NO_x in the tropical troposphere: A photochemical analysis of aircraft observations over the South Atlantic basin, *J. Geophys. Res.*, *101*(D19), 24,235–24,250.

Jacob, D. J., J. A. Logan, and P. P. Murti (1999), Effect of rising Asian emissions on surface ozone in the United States, *Geophys. Res. Lett.*, *26*(14), 2175–2178.

Jaeglé, L., L. Steinberger, R. V. Martin, and K. Chance (2005), Global partitioning of NO_x sources using satellite observations: Relative roles of fossil fuel combustion, biomass burning and soil emissions, *Faraday Discuss.*, *130*, 407–423, doi:10.1039/b502128f.

Jenkins, G. S., and J.-H. Ryu (2004a), Space-borne observations link the tropical Atlantic ozone maximum and paradox to lightning, *Atmos. Chem. Phys.*, *4*, 361–375.

Jenkins, G. S., and J.-H. Ryu (2004b), Linking horizontal and vertical transports of biomass fire emissions to the tropical Atlantic ozone paradox during the Northern Hemisphere winter season: climatology, *Atmos. Chem. Phys.*, *4*, 449–469.

Jonquières, I., and A. Marenco (1998), Redistribution by deep convection and long-range transport of CO and CH4 emissions from the Amazon basin, as observed by the airborne campaign TROPOZ II during the wet season, *J. Geophys. Res.*, *103*(D15), 19,075–19,092.

Jonquières, I., A. Marenco, A. Maalej, and F. Rohrer (1998), Study of ozone formation and transatlantic transport from biomass burning emissions over West Africa during the airborne Tropospheric Ozone cam-

paigns TROPOZ I and TROPOZ II, *J. Geophys. Res.*, *103*(D15), 19,059–19,074.
Krishnamurti, T. N., H. E. Fuelberg, M. C. Sinha, D. Oosterhof, E. L. Bensman, and V. B. Kumar (1993), The meteorological environment of the troposphere ozone maximum over the tropical South Atlantic Ocean, *J. Geophys. Res.*, *98*(D6), 10,621–10,641.
Krishnamurti, T. N., M. C. Sinha, M. Kanamitsu, D. Oosterhof, H. Fuelberg, R. Chatfield, and D. J. Jacob (1996), Passive tracer transport relevant to the TRACE-A experiment, *J. Geophys. Res.*, *101*(D19), 23,889–23,908.
Kunhikrishnan, T., and M. G. Lawrence (2004), Sensitivity of NO_x over the Indian Ocean to emissions from the surrounding continents and nonlinearities in atmospheric chemistry responses, *Geophys. Res. Lett.*, *31*, L15109, doi:10.1029/2004GL020210.
Labrador, L. J., R. von Kuhlmann, and M. G. Lawrence (2004), Strong sensitivity of the global mean OH concentration and the tropospheric oxidizing efficiency to the source of NO_x from lightning, *Geophys. Res. Lett.*, *31*, L06102, doi:10.1029/2003GL019229.
Lamarque, J. F., G. P. Brasseur, P. G. Hess, and J.-F. Mller (1996), Three-dimensional study of the relative contributions of the different nitrogen sources in the troposphere (1996), *J. Geophys. Res.*, *101*(D17), 22,955–22,968.
Lelieveld, J., et al. (2001), The Indian Ocean experiment: Widespread air pollution from South and Southeast Asia, *Science*, *291*(5506), 1031–1036.
Levelt, P. F., et al. (2006), The ozone monitoring instrument, *IEEE Trans. Geosci. Remote Sens.*, *44*, 1093–1101.
Liu, S. C., et al. (1987), Ozone production in the rural troposphere and the implications for regional and global ozone distributions, *J. Geophys. Res.*, *92*(D4), 4191–4207.
Liu, H., et al. (2006), Radiative effect of clouds on tropospheric chemistry in a global three-dimensional chemical transport model, *J. Geophys. Res.*, *111*, D20303, doi:10.1029/2005JD006403.
Liu, X., K. Chance, C. E. Sioris, R. J. D. Spurr, T. P. Kurosu, R. V. Martin, and M. J. Newchurch (2005), Ozone profile and tropospheric ozone retrievals from the Global Ozone Monitoring Experiment: Algorithm description and validation, *J. Geophys. Res.*, *110*, D20307, doi:10.1029/2005JD006240.
Logan, J. A., and V. W. J. H. Kirchhoff (1986), Seasonal variations of tropospheric ozone at Natal, Brazil, *J. Geophys. Res.*, *91*, 7875–7888.
Manning, M. R., D. C. Lowe, R. C. Moss, G. E. Bodeker, and W. Allan (2005), Short-term variations in the oxidizing power of the atmosphere, *Nature*, *436*, 1001–1004.
Martin, R. V., et al. (2002), Interpretation of TOMS observations of tropical tropospheric ozone with a global model and in situ observations, *J. Geophys. Res.*, *107*(D18), 4351, doi:10.1029/2001JD001480.
Martin, R. V., D. J. Jacob, R. M. Yantosca, M. Chin, and P. Ginoux (2003), Global and regional decreases in tropospheric oxidants from photochemical effects of aerosols, *J. Geophys. Res.*, *108*(D3), 4097, doi:10.1029/2002JD002622.
Martin, R. V., B. Sauvage, I. Folkins, C. E. Sioris, C. Boone, P. Bernath, and J. Ziemke (2007), Space-based constraints on the production of nitric oxide by lightning, *J. Geophys. Res.*, *112*, D09309, doi:10.1029/2006JD007831.
Marufu, L., F. Dentener, J. Lelieveld, M. O. Andreae, and G. Helas (2000), Photochemistry of the African troposphere: Influence of biomass-burning emissions, *J. Geophys. Res.*, *105*(D11), 14,513–14,530.
McLinden, C. A., S. C. Olsen, B. Hannegan, O. Wild, M. J. Prather, and J. Sundet (2000), Stratospheric ozone in 3-D models: A simple chemistry and the cross-tropopause flux, *J. Geophys. Res.*, *105*, 14,653–14,666.
Meyer-Arnek, J., A. Ladstatter-Weissenmayer, A. Richter, F. Wittrock, and J. P. Burrows (2005), A study of the trace gas columns of O_3, NO_2, and HCHO over Africa in September 1997, *Faraday Discuss.*, *130*, 387–405.
Moxim, W. J., and H. Levy II (2000), A model analysis of the tropical South Atlantic Ocean tropospheric ozone maximum, *J. Geophys. Res.*, *105*(D13), 17,393–17,416.
Newell, R. E. (1979), Climate and the ocean, *Am. Sci.*, *67*, 405–416.
Olsen, S. C., C. A. McLinden, and M. J. Prather (2001), Stratospheric N2O-NOy system: Testing uncertainties in a three-dimensional framework, *J. Geophys. Res.*, *106*, 28,771–28,784, doi:10.1029/2001JD000559.
Park, R. J., D. J. Jacob, B. D. Field, R. M. Yantosca, and M. Chin (2004), Natural and transboundary pollution influences on sulfate-nitrate-ammonium aerosols in the United States: Implications for policy, *J. Geophys. Res.*, *109*, D15204, doi:10.1029/2003JD004473.
Park, R. J., et al. (2005), Export efficiency of black carbon aerosol in continental outflow: Global implications, *J. Geophys. Res.*, *110*, D11205, doi:10.1029/2004JD005432.
Pickering, K. E., et al. (1996), Convective transport of biomass burning emissions over Brazil during TRACE A, *J. Geophys. Res.*, *101*(D19), 23,993–24,012.
Pickering, K. E., Y. S. Wang, W. K. Tao, C. Price, and J. F. Muller (1998), Vertical distributions of lightning NO_x for use in regional and global chemical transport models, *J. Geophys. Res.*, *103*, 31,203–31,216.
Price, C. J., and D. Rind (1994), Possible implications of global climate-change on global lightning distributions and frequencies, *J. Geophys. Res.*, *99*, 10,823–10,831, 97.
Price, C., J. Penner, and M. Prather (1997), NO_x from lightning: 1. Global distribution based on lightning physics, *J. Geophys. Res.*, *102*, 5929–5941.
Rodwell, M. J., and B. J. Hoskins (2001), Subtropical anticyclones and summer monsoons, *J. Clim.*, *14*(D19), 3192–3211.
Sauvage, B., V. Thouret, J-P. Cammas, F. Gueusi, G. Athier, and P. Nédélec (2005), Tropospheric ozone over Equatorial Africa: Regional aspects from the MOZAIC data, *Atmos. Chem. Phys.*, *5*, 311–335.
Sauvage, B., V. Thouret, A. M. Thompson, J. C. Witte, J-P. Cammas, P. Nédélec, and G. Athier (2006), "Tropical Atlantic Ozone Paradox" and "Zonal Wave-one" from the in-situ MOZAIC and SHADOZ Data, *J. Geophys. Res.*, *111*, D01301, doi:10.1029/2005JD006241.
Sauvage, B., R. V. Martin, A. van Donkelaar, X. Liu, L. Jaeglé, P. I. Palmer, and K. Chance (2007), Remote sensed and in situ constraints on processes affecting tropospheric ozone, *Atmos. Chem. Phys. Disc.*, *7*, 815–838.
Singh, H. B., et al. (1996), Impact of biomass burning emissions on the composition of the South Atlantic troposphere: Reactive nitrogen and ozone, *J. Geophys. Res.*, *101*(D19), 24,203–24,220.
Spivakovsky, C. M., et al. (2000), Three-dimensional climatological distribution of tropospheric OH: Update and evaluation, *J. Geophys. Res.*, *105*(D7), 8931–8980.
Thompson, A. M. (1992), The oxidizing capacity of the earth's atmosphere: Probable past and future changes, *Science*, *256*, 1157–1165.
Thompson, A. M., et al. (1996), Where did tropospheric ozone over southern Africa and the tropical Atlantic come from in October 1992? Insights from TOMS, GTE TRACE A, and SAFARI 1992, *J. Geophys. Res.*, *101*, 24251.
Thompson, A. M., B. G. Doddridge, J. C. Witte, R. D. Hudson, W. T. Luke, J. E. Johnson, B. J. Johnson, S. J. Oltmans, and R. Weller (2000), A tropical Atlantic paradox: Shipboard and satellite views of a tropospheric ozone maximum and wave-one in January–February 1999, *Geophys. Res. Lett.*, *27*, 3317–3320.
Thompson, A. M., et al. (2003), Southern Hemisphere Additional Ozonesondes (SHADOZ) 1998–2000 tropical ozone climatology: 2. Tropospheric variability and the zonal wave-one, *J. Geophys. Res.*, *108*(D2), 8238, doi:10.1029/2001JD000967.
Thornton, J., and J. P. D. Abbatt (2005), Measurements of HO2 uptake to aqueous aerosol: Mass accommodation coefficients and net reactive loss, *J. Geophys. Res.*, *110*(D8), D08309, doi:10.1029/2004JD005402.
Valks, P. J. M., R. B. A. Koelemeijer, M. van Weele, P. van Velthoven, J. P. F. Fortuin, and H. Kelder (2003), Variability in tropical tropospheric ozone: Analysis with Global Ozone Monitoring Experiment observations and a global model, *J. Geophys. Res.*, *108*(D11), 4328, doi:10.1029/2002JD002894.
Wang, Y., D. J. Jacob, and J. A. Logan (1998), Global simulation of tropospheric O_3–NO_x–hydrocarbon chemistry: 1. Model formulation, *J. Geophys. Res.*, *103*, 10,713–10,726.
Wang, P., J. Fishman, V. L. Harvey, and M. H. Hitchman (2006), Southern tropical upper tropospheric zonal ozone wave-1 from SAGE II observations, *J. Geophys. Res.*, *111*, D08305, doi:10.1029/2005JD006221.
Waters, J. W., et al. (2007), The Earth Observing System Microwave Limb Sounder (EOS MLS) on the Aura satellite, *IEEE Trans. Geosci. Remote Sens.*, in press.
Weller, R., R. Lilischkis, O. Schrems, and R. Neuber (1996), Vertical ozone distribution in the marine atmosphere over the central Atlantic Ocean, (56°S-50°N), *J. Geophys. Res.*, *101*(D1), 1387–1400.
Wu, S., L. J. Mickley, D. J. Jacob, J. A. Logan, and R. M. Yantosca (2007), Why are there large differences between models in global budgets of tropospheric ozone?, *J. Geophys. Res.*, *112*, D05202, doi:10.1029/2006JD007336.
Yamasoe, M. A., P. Artaxo, A. H. Miguel, and A. G. Allen (2000), Chemical composition of aerosols particles from direct emissions of vegetation fires in the Amazon basin: Water-soluble species and trace elements, *Atmos. Environ.*, *34*(10), 1641–1653.
Ziemke, J. R., S. Chandra, B. N. Duncan, L. Froidevaux, P. K. Bhartia, P. F. Levelt, and J. W. Waters (2006), Tropospheric ozone determined from Aura OMI and MLS: Evaluation of measurements and comparison with the Global Modeling Initiative's Chemical Transport Model, *J. Geophys. Res.*, *111*, D19303, doi:10.1029/2006JD007089.

R. V. Martin, B. Sauvage, and A. van Donkelaar, Department of Physics and Atmospheric Science, Dalhousie University, Halifax, NS, Canada. (bsauvage@fizz.phys.dal.ca)
J. R. Ziemke, Goddard Earth Sciences and Technology, University of Maryland Baltimore County, MD, USA.